Dynamic Electrostatic Confinement in an rf-Sustained Tandem Mirror

N. Hershkowitz, R. A. Breun, J. D. Callen, C. Chan, J. Ferron, S. N. Golovato, J. Pew, B. Nelson, D. Sing, and L. Yujiri

Nuclear Engineering Department, University of Wisconsin, Madison, Wisconsin 53706

(Received 9 August 1982)

Electrostatic ion confinement is demonstrated in an rf-sustained tandem mirror and shown to have a dynamic nature. Measurements of plasma potential and ion end loss on particular flux tubes show that confinement can be enhanced by a factor of 3 over direct-flow loss rates. The axial confining potential can vary with radial position and time resulting in changes in ion confinement with abrupt reductions in central-cell plasma density when axial potential confinement is reduced.

PACS numbers: 52.55.Ke, 52.55.Mg

The tandem mirror concept[1] appears to have many advantages for fusion reactors. In such devices a central-cell plasma in a solenoid is bounded by end cells. Plasma confined in minimum-$|B|$ magnetic mirror end cells provides magnetohydrodynamic (MHD) stability,[2] while tailoring of the magnetic field, fueling, and heating provide electrostatic ion and electron confinement. The tandem mirror experiment[3] (TMX) demonstrated electrostatic central-cell ion confinement by end-cell plasma potential barriers (plugs).

The ion potential barriers in the TMX experiment were produced by neutral-beam fueling and heating in the plugs. In the Phaedrus tandem mirror the plugs are heated by rf at the ion cyclotron resonance frequency ($\omega = \omega_{ci}$) and the central cell, by off-resonance rf heating ($\omega \lesssim \omega_{ci}$). The central cell is fueled by ionization of a hydrogen-gas puff and the plugs are fueled by rf trapping[4] of ions flowing from the central cell. In this paper we demonstrate that central-cell ions are electrostatically confined in this rf-sustained device. Direct measurements show that the confining potential varies radially and can also vary with time during a shot. The behavior of the ion end-loss rate and central-cell density are consistent with the confining potential. These results differ from the TMX results in which plasma parameters were relatively constant during the steady-state portion of a shot and the confining potential was constant across the central-cell radius.[3]

The Phaedrus tandem mirror[4,5] consists of a solenoidal central cell bounded by quadrupole minimum-$|B|$ mirror end plugs. The magnetic field is 2.6 kG at the plug midplane and 600 G in the central cell. The device can be operated with densities ranging from 0.7×10^{12} to 10^{13} cm^{-3}. The plasma radius (to e^{-1}) at the plug midplane was measured to be 5.5 cm which maps along a flux tube to 11 cm in the central cell. Typical electron temperatures are $T_e \approx 20$ eV and central-cell ion temperatures are $T_{ic} \approx 20$ eV. In the plugs $T_{ip} \lesssim 700$ eV.

The plasma potential was determined from the floating potential of collecting Langmuir probes in the central cell and self-emissive probes[6] in the plugs. In the central cell the bulk T_e was constant with radius. The difference between the plasma and floating potentials was also found to be independent of radius and equal to 30 ± 5 V so that the floating potential of 0.1-cm-diam platinum spheres was used to obtain measurements of the plasma potential. In the plugs, a hot-electron tail results in a floating potential for a collecting probe of -500 V while the plasma potential is typically $+70$ V. The difference between the floating and plasma potentials was found to vary with radius. Therefore, measurements of the plug plasma potential were carried out with self-emissive probes[6] for which the floating potential approximately equals the plasma potential. The probes consisted of 0.25-mm-diam, 2-mm-long thoriated tungsten wires which were heated to electron emission by the collected ion current. Simultaneous data were taken at the plug midplane with three probes mounted 2.5 cm apart radially and in the central cell with three probes located on the same flux tubes as the plug probes. We will refer to all radial coordinates in terms of the corresponding coordinates at the plug midplane. Line densities were measured with 70-GHz microwave interferometers at the midplanes of the plugs and the central cell.

At the beginning of a shot the plasma potentials depend on the amount and timing of the central-cell gas puff and on the plug rf field strength. When the initial plug potential φ_p is equal to or exceeds the central-cell potential φ_e we find that

the plasma can be rf sustained. However, if $\varphi_p \gg \varphi_e$, the plug presents a large potential barrier to the central-cell ion stream so that ions are well confined in the central cell and do not reach the rf resonance in the plugs. This limits the plug fueling rate which leads to a rapid decay of the plug density n_p and to increases in the central-cell density n_c when the stream gun is turned off. It is possible to reach an equilibrium with n_c approaching n_p and the plasma can sustain for up to 25 msec.

The plasma potential was found to be "hollow" in both the central cell and the plugs. At a given axial position, the potential was everywhere positive but usually had a minimum value on axis and a maximum positive value at larger radii. This is probably due to direct rf heating of electrons[7] by the rf fields which are stronger near the plasma edge. On some flux surfaces the difference between plug and central-cell potentials ($\varphi_c \equiv \varphi_p - \varphi_e$) was found to be ion confining ($\varphi_c > 0$). The value of φ_c usually increased with radial position but we observed that it varied from shot to shot and even during a given shot. In Fig. 1 we give data for a representative shot which sustained for 18 msec with relatively little variation in φ_p, φ_e, and φ_c. Figure 1(a) shows that the plug density, n_p (computed from the measured line density), closely follows the central-cell density, n_c, for the first 7 msec. After 7 msec, n_p/n_c increases, reaching a maximum of more than 2 at 17 msec. If we assume that φ_c is related to the densities by $n_p/n_c \approx \exp(e\varphi_c/T_e)$, that T_e is uniform, and that radial density profiles are similar in the plug and central cell, the data in Fig. 1(a) indicate that the ion confining potential should never exceed $0.7T_e/e \approx 14$ V. The data in Fig. 1(b) show that at some locations larger ion confining potentials ($\varphi_c \sim 35$ V) existed during this shot, but that φ_c was not constant with radius. Near the axis φ_c was negative except for the last 2 msec so that central-cell ions were not electrostatically confined on axis during most of the shot. On the other hand, at $r = 3.5$ cm the potential difference became positive at 5 msec and continued to be ion confining for the remainder of the shot. At $r = 6$ cm, the plug emissive-probe data are only available after 7 msec but by then the potential difference was approximately 30 V positive. Throughout most of this shot, plasma was electrostatically confined in the region away from the axis. From this example, it is apparent that computations of φ_c based on line density give values which do not necessarily apply on individual flux tubes but which may be representative of the average value of φ_c.

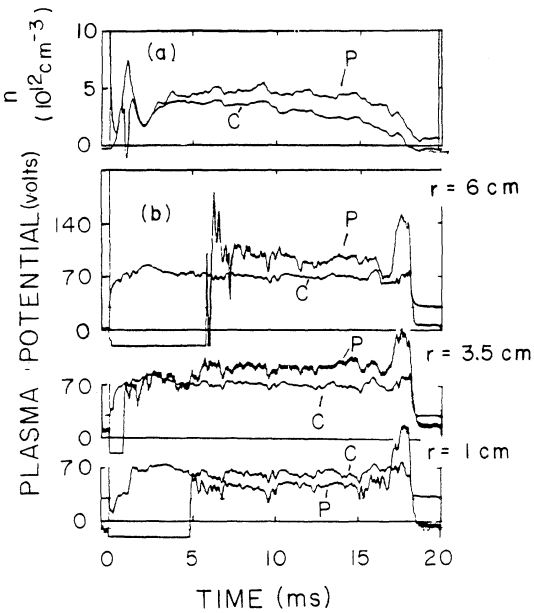

FIG. 1. Plasma parameters during a shot with relatively constant confining potential. (a) Plug and central-cell peak density computed from the measured line density. (b) Plasma potential in the plug and central cell.

During shots when the plasma potentials vary in time the self-consistent behavior of the axial ion loss rate demonstrates the presence of central-cell ion confinement by potential barriers. An example is given in Fig. 2. The central-cell density shown in Fig. 2(a) exhibits a staircaselike structure with sharp discontinuities at 7 and 10 msec. We can account for these sharp decreases in density by examining the time dependence of the plasma potentials shown in Fig. 2(b). Comparison of the central-cell potential data at three radii show that φ_e again tends to be hollow. For example, at $t = 2.5$ msec the values at $r = 0$, 2.5, and 5 cm are 63, 77, and 82 V, respectively. The overall central-cell potential is seen generally to decrease slowly for the first 7 msec and then to increase, while the plug potential undergoes large variations during the entire shot. This causes φ_c to vary over a wide range. Unlike the data shown in Fig. 1, the initial potential is seen to be ion confining on axis and at $r = 2.5$ cm. However, φ_c decreases and reaches *negative* values at $t \approx 7$ msec. Then it increases, reaching a maximum value of approximately 40 V at 9 msec and 2.5 cm. It then decreases again, reaching values close to zero at $t \approx 10$ msec. The abrupt changes in density correlate with the en-

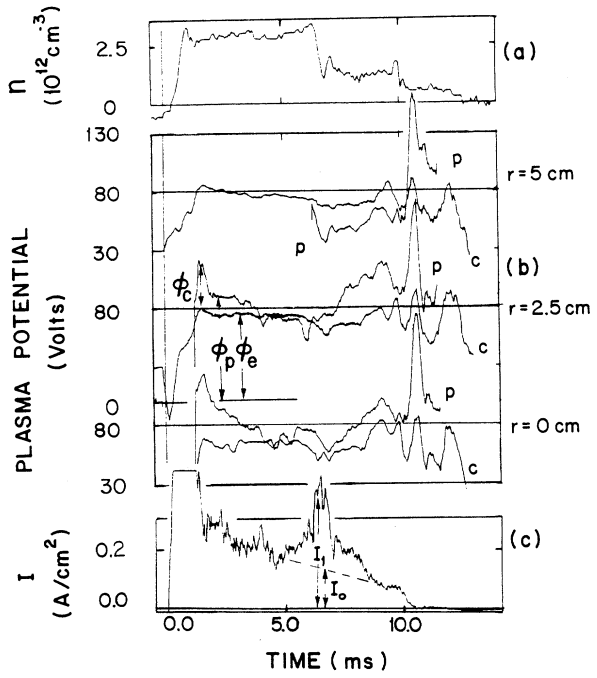

FIG. 2. Plasma parameters during a shot with time-varying potential levels. (a) Central-cell peak density computed from the measured line density. (b) Plasma potential at three radii in the plug and central cell. (c) Ion-loss current density at the plug midplane as measured by an ion end-loss collector located on a flux tube mapping to $r=3.5$ cm in the plug and $r=7$ cm in the central cell. I_1, the current in the absence of a confining potential, is determined from the peak at 7 msec, the collector area (0.28 cm^2), and the ratio of the magnetic field strength at the plug midplane to the strength at the analyzer (5.2).

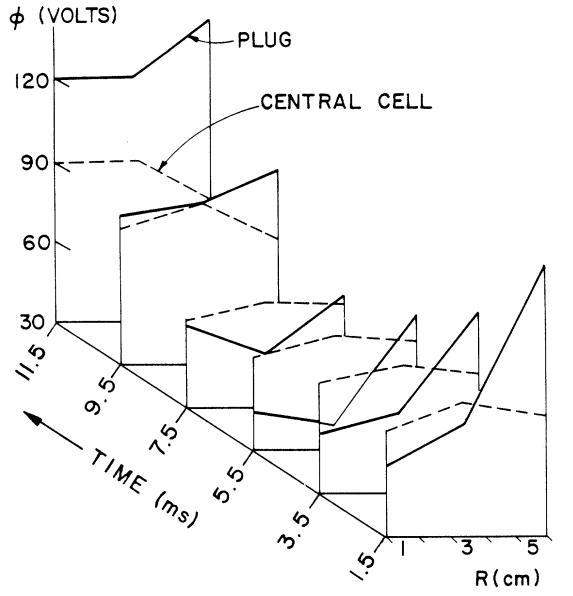

FIG. 3. The plasma potentials in the plug (solid lines) and central cell (dashed lines) vs plug radial position and time.

hanced axial ion end loss shown in Fig. 2(c). Note that the ion dump and the sharp density changes occur simultaneously with minima in φ_c indicating that a reduction in ion confining potential during the shot results in increased ion end loss.

We can make use of the data in Figs. 2(a) and 2(c) to determine approximate values for $e\varphi_c/T_{ic}$ and the central-cell ion particle confinement time τ_0 corresponding to $\varphi_c=0$. The steady-state central-cell loss current can be written[3] $I=n_c{}^2V/n_c\tau$, where $n_c\tau$ depends on the value of φ_c/T_{ic}. For $\varphi_c/T_{ic}=0$,

$$n_c\tau_0=n_c\tau_{ii}\ln R_c+2n_cL_c(\pi M_i/8T_{ic})^{1/2}R_c, \quad (1)$$

and

$$n_c\tau_c=\left[5.5\times10^5T_{ic}{}^{3/2}H(R_c)K\left(\frac{\varphi_c}{T_{ic}}\right)+2n_cL_c\left(\frac{\pi M_i}{8T_{ic}}\right)^{1/2}\frac{R_c}{R_p}\right]\exp\left(\frac{\varphi_c}{T_{ic}}\right) \quad (2)$$

for $\varphi_c/T_{ic}\gtrsim 1$. Here $R_c=7.5$ and $R_p=1.7$ are the central-cell and plug mirror ratios, $L_c=230$ cm is the central-cell length, H and K are factors of order 1 for the parameters of this experiment, and M_i is the ion mass. The first term in both expressions is the Pastukhov loss time which is small in our experiment compared with the second term, the collisional loss time. Therefore, the ratio of loss current during the ion dump (when $\varphi_c=0$), I_1, to steady-state loss current is approximately $I_1/I_0=R_p{}^{-1}\exp(e\varphi_c/T_{ic})$. The experimental value for this ratio from Fig. 2(c) is $I_1/I_0\approx 3$ so that $e\varphi_c/T_{ic}\approx 1.6$ in agreement with Fig. 2(b). This indicates that the plug potential barrier is providing a factor-of-3 reduction in the steady-state end loss.

We can approximate τ_0 by the density decay rate during the period of the sharp density drop, when $\varphi_c=0$. This gives $\tau_0\approx 0.4$ msec. A value of τ_0 can also be computed during this time period for the flux tube which maps into the end-loss collector for which data are shown in Fig. 2(c). Use of $\tau_0=I_1/nV$, with the central-cell density in the flux tube (computed from the line density under the assumption of a Gaussian profile) $n=1.8\times10^{12}$ cm^{-3}, flux tube volume $V=65$ cm^{-3}, and peak current measured at the end loss analyzer $I_1=23.5$ mA, gives $\tau_0=0.4$ msec. A theoretical estimate of τ_0 obtained from Eq. (1) gives $\tau_0=0.5$ msec

which agrees well with the experimental results.

Figure 3 shows plasma-potential radial profiles in the plug and central cell for another shot where the potentials vary over a wide range. Early in the shot the radial electric field is relatively large with $\varphi_c < 0$ for $r < 3.5$ cm. The ion confining potential is seen to decrease and reach a minimum with $\varphi_c < 0$ out to 5.5 cm. It then increases and $\varphi_c > 0$ for all radial positions later in the shot. Note that in this case φ_c has minima off axis and that the radial electric field varies in time and in fact can change direction.

In conclusion, we have given the first demonstration of electrostatic ion confinement in an rf-sustained tandem mirror. Ion confinement was observed to be enhanced by up to a factor of 3 on individual flux tubes. The radial potential profile was found to be hollow. This could result in radial transport which is quite different from that in a neutral-beam–sustained device where the potential is peaked on axis. It was also shown that ions can be confined off axis when there is no electrostatic confinement on axis in contrast to the TMX results where the axial confinement was independent of radius. The confinement was shown to be dynamic in the sense that the plasma can adjust to large central-cell density losses and again find ion-confining configurations with $\varphi_c > 0$. This ability to adjust to changes in parameters appears to be characteristic of an rf-sustained tandem mirror, in which plug fueling by rf trapping is coupled to the central-cell density and confining potential.

This work was supported by U. S. Department of Energy Contract No. DE-AC02-78-ET51015.

[1]G. I. Dimov, V. V. Zakaidakov, and M. E. Kishinevsky, Fiz. Plazmy 2, 597 (1976) [Sov. J. Plasma Phys. 2, 326 (1976)]; T. K. Fowler and B. G. Logan, Comments Plasma Phys. Controlled Fusion 2, 167 (1977).

[2]A. Molvik *et al.*, Phys. Rev. Lett. 48, 742 (1982), and references contained therein.

[3]F. H. Coensgen *et al.*, Phys. Rev. Lett. 44, 1132 (1980); T. C. Simonen *et al.*, Lawrence Livermore Laboratory Report No. UCRL-53120, 1981 (unpublished); D. L. Correll *et al.*, Nucl. Fusion 22, 223 (1982).

[4]R. A. Breun *et al.*, Phys. Rev. Lett. 47, 1833 (1981).

[5]R. A. Breun *et al.*, in *Proceedings of the Eighth International Conference on Plasma Physics and Controlled Fusion Research, Brussels, 1980* (International Atomic Energy Agency, Vienna, 1981), p. 105.

[6]J. R. Smith, N. Hershkowitz, and P. Coakley, Rev. Sci. Instrum. 50, 210 (1974); N. Hershkowitz *et al.*, University of Wisconsin Report No. PTMR 82-6 (unpublished).

[7]D. K. Smith and B. McVey, Bull. Am. Phys. Soc. 27, 915 (1982).